Neutral Gas Effects on the Charging of ECHO-7

P. R. Malcolm
Department of Physics
USAF Academy, CO 80840

and

W. J. Burke and G. P. Murphy
Geophysics Laboratory (AFSC)
Hanscom AFB, MA 01731-5000

ABSTRACT

Electron beams reaching 40 KeV in energy and 220 milliamperes in current were emitted during the ECHO-7 sounding rocket flight. In order to measure the potential of the beam emitting MAIN payload, a high impedance probe (TETHER) was ejected from MAIN near apogee (292 km). During the flight, beam emission frequently occurred together with attitude control system (ACS) corrective maneuvers involving the ejection of nitrogen gas. Four seconds of data from the tether and an upward looking surface current monitor (SCM), located at the gun end of the payload, show the effects of ACS neutral gas on the current/voltage characteristics of the MAIN payload.

During beam emission with no ACS gas ejection, the tether measured charging levels of 2-3 kilovolts while the SCM measured current densities of 8-10 microamperes/cm^2. Then during all simultaneous electron beam and ACS emission periods, the vehicle potential decreased to a few tens of volts and the SCM detected only background level return currents. When ACS gas ejection across magnetic field lines terminated, the vehicle potential and SCM current immediately returned to their original values (2-3 kV, 8-10 μA). In contrast, gas ejected with velocity components along the magnetic field lines continued to influence the vehicle potential for several tens of milliseconds after the flow was turned off. In this case, vehicle potentials were below while the SCM currents were above their original values with no ACS gas ejection. These results are consistent with the return current being localized to the immediate vicinity of the emitting ACS nozzles and show the strong influence of the earth's magnetic field on the motion of the return current electrons.

INTRODUCTION

On the evening of February 8, 1988, at 8:16:49 UT, the ECHO-7 sounding rocket payload was launched toward the east from the Poker Flat Research Range. ECHO-7 was a sophisticated experiment designed to study the complex interactions of artificial electron beams propagating great distances along magnetic field lines in space (Winckler et al , 1989). It is known that energetic electron beams interact with themselves, the space environment and their host vehicles. This report concentrates on the interactions in the immediate vicinity of the ECHO-7 beam-emitting MAIN payload during a four second period near its 292 km apogee. During this interval, we measured how the vehicle potential responded to several different types of beam operations by means of a high-impedance tethered probe. Of particular interest are the dynamics of the vehicle potentials and return currents following intermittent emissions of neutral gas from the payload's attitude control system (ACS). Unfortunately, the tether voltage measurements were prematurely terminated by a nearly catastrophic event that destroyed the power convertor for several diagnostic sensors and triggered a safety circuit that temporarily shut down beam emissions (Malcolm et al., 1989).

Beam-induced spacecraft anomalies are well known hazards of the trade. During an electron beam emission operation on the SCATHA (P78-2) satellite, severe arcing was induced, an energetic electron spectrometer was destroyed and the main telemetry system was temporarily impaired (Cohen et al., 1981). At the time of these upsets the beam energy and current were 3 keV and 13 mA (39 W), respectively. Data from the Norwegian rocket MAIMIK indicate that whenever currents from its 8 kV gun exceeded 84 mA (640 W) the vehicle charged to at least beam energy (Maehlum et al., 1988). During one MAIMIK charging event, a spurious command was induced causing a pyrotechnic device to detonate prematurely. During the BERT-1 sounding rocket flight, the main telemetry encoder and the experiment sequencer were destroyed when the payload's electron gun was turned on with beam energy and current of 2 keV and 20 mA (40 W). Most recently, when the SCEX-2 electron beam system was turned on, arcing from 170 volt battery packs to payload ground resulted in their destruction during flight (Massey et al., 1987).

None of these are cases of human carelessness. In all cases, the beams systems were tested in laboratories for many hours prior to flight. Rather, these failures testify to the inherently hazardous conditions that develop whenever energetic particle beams are emitted into space plasmas. Because particle beams offer powerful methods for actively

probing space plasmas, it is imperative to consider carefully the circumstances surrounding all beam-induced spacecraft interactions.

Recently Banks et al. (1988) reported on the results of the CHARGE-2 sounding rocket experiment, a tethered mother-daughter payload that emitted a 1 keV electron beam with currents up to 40 mA. The potential of the mother was normally high. However, whenever gas was released from the ACS on the tethered daughter vehicle, the potential of the mother decreased dramatically. This indicates that ionization of neutral gas during ACS releases increases the source for neutralizing current, thus reducing the required vehicle potential. Within certain environments this may provide a simple and safe technique for assisting energetic electron beams in escaping from emitting bodies in space with little energy degradation.

This report is divided into three main sections in which we first summarize the ECHO-7 mission and its payload complement. We next give a detailed presentation of vehicle potential and return current measurements acquired during a four second period which included a sequence of planned beam emissions and random neutral gas releases. Finally we discuss elements of a simple, empirical model that qualitatively helps us understand the interactions.

MISSION AND PAYLOAD

The main purpose of the ECHO-7 experiment was to study the propagation characteristics of energetic electron beams travelling great distances along magnetic lines of the earth (Winckler et al., 1989). During the experiment, electron beams were emitted from the MAIN payload flying over Alaska. Guided by the earth's magnetic field, the beams propagated to the southern ionosphere to the west of Antarctica. There, they either magnetically mirrored or were scattered off the atmosphere. Upon reflection to the northern hemisphere, the electrons were detected by sensors deployed on or near the beam-emitting vehicle (Winckler, et al., 1989, Nemzek, 1990 and Nemzek, et al., 1991). The time delay between beam emission and the detection of electron echoes has been used to calculate the shapes of field lines threading the distant magnetosphere (Nemzek, 1990 and Nemzek, et al., 1991). To understand the observations it is critical to know the energy of the electrons after they leave the immediate vicinity of the emitting payload.

Secondary objectives of the mission include the investigation of how charged particle beams interact with the ionospheric plasma environments and with their host

vehicles. Environmental effects include the ionization/excitation of atmospheric and host-vehicle neutrals, and collective interactions with charged particles in the beam or ionospheric plasma. Interactions with neutrals manifest themselves mostly through the emission of light. Beam plasma interactions lead to the emission of electrostatic and/or electromagnetic waves in the VLF and HF frequency bands. The most important interaction with the host vehicle involves surface charging and the development of high potential sheaths.

Figure 1 sketches the configuration of the ECHO-7 science payload. The instrumented nosecone section (NOSE), ejected within a few degrees of the magnetic field line, was primarily designed to detect waves generated in or near the beam. The Plasma Diagnostics Package (PDP) was ejected magnetically south while the Energetic Particles Payload (EPP) was ejected to the magnetic north-west of the beam-emitting MAIN payload. They each carried sensors to detect echoing, energetic electrons and beam-related electromagnetic fields. The PDP also carried a low-light level television camera that pointed back along the PDP spin axis toward the position of the MAIN. Detailed descriptions of the NOSE, PDP and EPP complement of instruments have been written by Winckler et al. (1989) and are not needed for the present study. In what follows we concentrate on the MAIN payload's instrumentation and operations.

The MAIN payload consisted primarily of an electron accelerator, scientific instrumentation, a telemetry system and an attitude control system (ACS). The ACS used pressurized nitrogen with pitch, roll and yaw jet nozzles to maintain three-axis stability. The positions of the jets relative to the magnetic field direction are shown in Figures 2 and 3. They were located about 1.5 m aft (south) of the electron gun aperture. After initial payload deployments, gas emissions occurred randomly throughout the flight to keep the orientation of MAIN perpendicular to the earth's magnetic field.

The ECHO-7 9 kW electron beam accelerator is shown schematically in Figure 4. It functioned perfectly from turn-on at 179 sec (250 km) through reentry at 500 sec (90 km) while emitting beams reaching 40 keV in energy and 220 mA in current. The accelerator was similar to those flown on previous ECHO missions, but incorporated several design changes to increase program flexibility and reliability. It had five basic components: a battery power system, power converters, a diode electron emitter or gun, beam focusing and deflection magnets, and a programmer to control functions during flight.

Primary power was supplied by four silver-zinc battery packs capable of delivering up to 100 volts at 100 amperes when connected in series. Power was taken from one of two battery taps selected by the programmer. The high voltage tap was connected to the top of the 100 volt (loaded) pack while the low tap connected to a point capable of delivering 25 volts under load. This power fed the primary side of a DC-DC converter that stepped the 100 volts up to 40 kV with a maximum current of 250 mA. This produced a DC output with < 10 percent ripple (see Figure 5, "Discrete Mode"). No attempt was made to filter the output because of the hazards involved in using large capacitors charged to high voltages.

A second, or "continuous", accelerator mode used the converter drive to charge and discharge a 500 μF capacitor during each drive cycle. When the transformed output was full wave rectified, the resultant output decayed exponentially from 40 kV to 8 kV during each millisecond half-cycle (see Figure 5, "Continuous Mode"). This mode is called "continuous" because it results in an electron beam continuously spread in energies between 40 and 8 keV. Continuous mode beams were used to enhance the probability of echo detection (Winckler et al., 1989).

The electron gun was a space-charge limited diode with a geometry described by Pierce (1949). The source of electrons was a tantalum ribbon filament heated to incandescence with a floating power supply. The filament and cathode focusing element were biased by the negative high-voltage output of the accelerator convertor while the gun anode was grounded to the payload skin. Since the gun was not emission limited within its operating range, it was capable of producing a beam current of 220 mA with a -40 kV bias and 30 mA with a -10 kV bias, following the $V^{3/2}$ relation for a space-charge limited diode.

The accelerator was placed in the payload so that when the MAIN was stabilized perpendicular to the earth's magnetic field, with the long axis parallel to the magnetic north-south direction, the electron beam injection pitch angle with no magnetic deflection was 110°. In the "continuous" accelerator mode the beam always emitted at a pitch angle of 110°. With the deflection magnet turned on, other injection pitch angles were possible when the accelerator was in the "discrete" mode. These were downward at a pitch angle of 40°, upward at a pitch angle of 170° and a continuous sweep from 40° to 175°.

All the accelerator emission modes and beam-deflection angles were controlled by a simple programmer interfaced to the accelerator drive circuits through fiber-optic links for maximum noise immunity. A 200-step accelerator program was

burned into EPROMs that were read every 50ms in a program of 10 second duration. Figure 6 shows that the program consisted of "discrete" injections at two different energies and four series of coded pulses in the "continuous" mode. The code consisted of a mix of 50, 100 and 150 ms duration pulses that allowed identification of exactly which pulses were detected as conjugate echoes.

Care was taken to prevent catastrophic damage to the power convertor system if high-voltage breakdown in the gun should occur. A safety circuit was designed to monitor the battery current and to inhibit the accelerator convertor for 300ms if the primary current exceeded 100 amperes. It did not, however, affect the precise 10 second repetition rate of the programmer. The safety circuit saved the drive system from three potential failures during flight when breakdowns occurred within the gun (Malcolm et al., 1989).

Besides the electron accelerator, the MAIN payload carried a tethered probe (TETHER) to measure the potential of the MAIN during beam operations, a set of photometers, a set of scintillator electron detectors, a complement of Geiger-muller tubes, two electrostatic analyzers (ESA) and a bipolar, 1 cm^2 surface-current monitor (SCM). The SCM and the ESAs were located at the top (north) end of the MAIN and looked directly up the magnetic field lines. This paper makes extensive use of simultaneous data from the TETHER and the SCM whose measurements were sampled 625 times per second.

The time-altitude plot in Figure 7 shows the TETHER being ejected near apogee (279 seconds, 292 km). It was spring ejected with a velocity of about 1.5 meters per second in the magnetic north direction. Sixty meters of Teflon insulated wire, stored on a fishing reel inside the probe, played out as the probe moved northward. Images from the PDP television camera showed that the probe succeeded in reaching its full 60 meter separation distance and rebounded back towards the MAIN near the end of the flight. The TETHER probe itself was an Aerodag coated aluminum cylinder with a total surface area of 544 cm^2. The probe was electrically connected to an isolation amplifier in the MAIN through a 10^9 Ohm resistor (see Figure 8). The circuit was designed to measure potential differences at three levels of sensitivity up to 5kV. To provide an in-flight calibration of the TETHER current collection system, the reference of the isolation amplifier was tied to stepping power supply that periodically biased the system at 100, 200, 300, 400 and 500 volts.

PAYLOAD POTENTIAL AND RETURN CURRENT VARIATIONS

In this section we consider the vehicle responses to various combinations of beam emissions and ACS maneuvers during the period in which the tethered probe was operating. An overview of measurements retrieved during the period from 278.5 to 283.5 seconds is given in Figure 9. The top three panels of the figure give the on/off status of the pitch, roll and yaw ACS jets. The next two panels give the potential between the MAIN and the TETHER on scales of 0 - 5000 volts and 0 - 1000 volts, respectively. The sixth panel indicates negative biases between 0 and 500 volts applied to the TETHER in 100 volt increments. The bottom two panels show the energy and pitch angles of the emitted beams.

Due to the impulse associated with the ejection of the TETHER at 279 seconds, a large number of ACS ejections occurred in the following 1.5 seconds. A cursory glance at the TETHER voltage measurements during the first sequence of continuous beam operations (when ACS activities were frequent) and the second sequence (when ACS activities were infrequent) reveals significantly different responses. Exact details are examined below. We note that during the early phase (280.35-280.75 sec) of the 10 keV emission, the vehicle potential was approximately 350 volts. Except at the time of the pitch maneuver near 281.1 sec, the potential difference between the TETHER and the MAIN increased with the applied biases. We also note that during the 36 keV operations the TETHER potential was generally in excess of the 5 kV measurable potential. During the downward emission near 282.85 sec the TETHER potential hovered very close to 5 kV.

A comparison of the actual with the planned operations (Figure 6) shows that the 110°, 36 keV beam emission near 283.1 sec terminated early and the planned upward injection never occurred. This beam turn-off was associated with an ejection of gas from one of the pitch ACS jets during which the power convertor for the TETHER and the surface current monitor was destroyed. The beam turn-off was caused by the activation of the safety circuit when the primary of the beam power drive tried to draw current in excess of 100 amperes. Malcolm et al. (1989) showed that this demand for high currents was caused by a breakdown due to the presence of positive ions within the gun. We note that all three cases of safety circuit activation coincided with ACS releases and occurred when the deflection magnetic field was either off or weak. The latter point suggests that the damaging ions were created outside of the gun aperture. This is also supported by pre-flight vacuum chamber tests of the accelerator system. During those tests, breakdown

occasionally occurred within the gun when the beam deflection magnet was turned off or was at a low field strength.

Before considering detailed responses of the vehicle to gas releases during continuous operations, it is useful to consider first the situation when no gas releases occurred. Figure 10 gives data acquired during a 50 ms continuous beam emission beginning at 282.353 sec. The top three panels show that all jet nozzles were closed. The vehicle potential, measured at three levels of sensitivity are given in the panels marked HVM3, HVM2, and HVM1 with full range deflections of 0 to 100 volts, 1000 volts and 5000 volts, respectively. The panel marked HVM4 gives the current measured by the 1 cm^2 surface current monitor. This sensor measured background electron current densities (toward the vehicle) of about $4x10^{-8}$ amperes/cm^2. Note that this "background" level is about 40 times higher than that provided by the natural, diffuse auroral precipitation in which the payload flew. The voltage monitor shows that in the 15 ms after gun turn-on the MAIN acquired a potential of 3.8 kV that gradually decreased to 2.5 kV. The current measured by the surface current monitor was about 8 μA. This was typical of measurements during other continuous beam operations with no ACS activity.

The estimated return current density for the continuous injections was estimated by dividing the average current during continuous injections (I_{ave} = 64 mA) by the effective area of the MAIN payload perpendicular to the magnetic field (Aperp = 0.9 m^2). The estimated current density is about 4 μA/cm^2. If the return current had access to only one side of the payload, the current density would obviously be 8 μA/cm^2, nearly the same as the measured current.

The mean and standard deviations of the potential and the SCM measurements during discrete emissions with no ACS gas or biases are listed in Table 1.

TABLE 1

Beam Operation	MAIN Potential (volts)	Surface Current (μA/cm^2)
10 keV, 30 mA	347 +/- 38	3.2 +/- 0.4
36 KeV, 185 mA, up	~ 5,000	8.4 +/- 1.4
36 keV, 185 mA, out	> 5,000	11.6 +/- 4.8

The first example of the effects of ACS gas releases, during a 100 millisecond continuous electron gun operation beginning at 279.533 sec, is given in Figure 11. The beam

ejection was preceded by bursts from the pitch jets, beginning at 279.507 sec and ending at 279.550 sec. After beam turn-on, the MAIN potential only went to 35 V and the current measured by the SCM remained at its background level. When the pitch jets turned off, the potential of the MAIN quickly increased to more than 2 kV and the SCM detected currents in the 8 to 10 μA range. The roll jet opened at 279.565 and closed at 279.600 sec. Again the vehicle potential decreased to about 30 V and background currents at SCM. However, after the gas turned off, the potential and currents remained at depressed levels for 33 ms until the gun operation terminated.

Figure 12 provides a second example, this time with gas coming from the upward pointing yaw jet. While the beam and jet were both turned on, the vehicle potential was about 60 volts and SCM measured background level currents. In the 25 ms after the yaw jet nozzle closed, the vehicle potential and SCM current increased to 600 volts and more than 10 μA, respectively.

The final example, Figure 13, is designed to show the persistence of gas from ACS roll maneuvers. After the first beam turn-on at 279.233 sec, the potential and current monitors measured values > 2 kV and 10 μA. When the nozzles opened they decreased to 45 volts and background, respectively. After a 50 ms gun-off interval, the beam turned on for a 100 ms operation. Lingering effects of the gas are evident. We see that the potential of the MAIN slowly increased to 1.5 kV, a full kilovolt below the average charging level for continuous emissions with no ACS gas. The current collected at SCM reached values of 16 μA, almost twice the amount collected in the example shown in Figure 10.

For the sake of comparison we have plotted in Figure 14 the current measured by the SCM as a function of vehicle potential. The circled dots represent all of the data points measured subsequent to the turn-off of the yaw jets (Figure 12). The "x" points were measured in the 100 msec period after 279.333 sec (Figure 13). Measurements taken during the discrete operations, summarized in Table 1, and the continuous operation (C) shown in Figure 10 are also plotted. The lowest voltages and currents were detected after nozzle turn offs. Although the vehicle potentials did not recover to the levels without gas, the highest currents measured by SCM occurred after gas ejections. The straight lines in Figure 14 representing $I \alpha V^{n/2}$, where n = 1, 2, 3 are meant as guides for the eye to which we attribute no physical significance at this time.

DISCUSSION

The results of the previous section can be summarized in terms of three empirical conclusions:

(1) During all types of ACS releases, the vehicle potential decreased to between 30 and 60 volts and the SCM measured currents at background levels.

(2) Immediately after pitch ACS maneuvers the vehicle potential and the SCM measurements returned to levels associated with no gas near the MAIN.

(3) For several tens of milliseconds after yaw and roll maneuvers the vehicle potential remained depressed but return current at the SCM exceeded unperturbed values.

In the following paragraphs we discuss the significance of these results for our understanding of beam vehicle interactions during and after ACS gas releases at ionospheric F-layer altitudes.

The decreased potentials of MAIN with respect to TETHER during ACS operations agrees with the results from CHARGE 2 reported by Banks et al. (1988). This general result was theoretically anticipated by Linson (1983), although he had the case of outgassing from the Shuttle in mind. The consistent measurement of low return-current readings by SCM at first appears counter intuitive. With the vehicle potential lowered from 2 - 3 kV to several tens of volts, the beam more easily escapes through the sheath surrounding the MAIN. Thus, total return currents equivalent to the full beam current must be collected on the surface of MAIN. These return currents are made up of electron extracted from the nearby atmosphere and newly produced ionization from the ACS gas plumes. The non-detection of return current electrons by the SCM provides a critical clue about the nature of plume-vehicle interactions.

We recall that the SCM was a 1 cm^2 patch that looked upward along the magnetic field and located on the north end of MAIN, close to the location of the electron gun aperture. The ACS jets were on the south end of the payload, about 1.5 meters aft of the gun and SCM. During ACS releases, most of the return current was not collected at the beam end of the vehicle. The surface collecting area of MAIN was approximately 3 m^2. During discrete 10 and 36 keV operations the gun emitted 30 and 180 mA, respectively. If current was uniformly collected on the surface of MAIN, SCM would have detected 1.6 and 7.2 μA, about a factor of two lower than levels in Figure 14. We attribute this to the

control of electron motion exerted by the earth's magnetic field.

Scaling the "c" data points in Figure 14, we estimate a root mean squared current of approximately 100 mA during continuous emissions. During ACS releases, N_2 molecules were released at the rate of ~ 10^{23} per second. Providing a return current of 100 mA required the ionization of only one molecule in 10^5. The several tens of volts detected during gas emissions is sufficiently above the 15.5 eV ionization potential of N_2 to generate the required current.

The fact that currents detected at the location of SCM remained at background levels during gas releases is consistent with the bulk of the return current being collected close to the locations of the ACS jets. The probability of producing ionizing collisions between ambient electrons and neutral molecules is greatest close to the jet where the densities of emitted, neutral molecules and the kinetic energies of impacting electrons are highest. Also, for an electron to contribute to the return current it must be allowed access to the surface by the earth's magnetic field. At auroral latitudes the gyroradius of a 10 eV electron is about 20 cm.

The influence of the earth's magnetic field explains the varied current/voltage responses of the MAIN after gas emissions from the different jets terminated. Figures 2 and 3 show that the pitch nozzles ejected gas across the magnetic field, while the gas from the roll and yaw jets had significant components along the earth's field. Data in Figure 11 show that as soon as the pitch jet turned off the vehicle potential and the return current collected by the SCM returned to their unperturbed values. Electrons created in the N_2 cloud after it magnetically separated from the MAIN could not return in large numbers to the vehicle's surface. In the cases of roll and pitch ejections the gas remained in magnetic contact with the vehicle for relatively long periods of time after gas turn-off. Significant fractions of the electrons created in ionizing interactions within these clouds (with accelerated ambient or beam electrons) maintained access to the vehicle's surface, but now in the vicinity of SCM.

CONCLUSIONS

We conclude that in the light of our experience with
ECHO 7, the suggestion of Banks et al. (1988) that neutral
gas emissions provide a safe method for ensuring that
energetic beam particles get away from the emitting vehicle
should be qualified. First, if possible, use continuous gas
emissions to protect the vehicle from very rapid changes in
charging status. Second, if only intermittent gas releases
are possible, deflection magnets can protect the gun from
internal discharges. Third, the effects of intermittent
gas releases can be enhanced by directing them with a thrust
component in the direction of the magnetic field.

REFERENCES

Banks, P.M., B.E. Gilchrist, T. Neubert, R.I. Bush, P.R. Williamson, N. Meyers and W.J. Raitt, Rocket observations of electron beam experiments with vehicle charging neutralized by neutral gas plumes, XXVII COSPAR, 18 - 29 July 1988, Espoo Finland, Topical Meeting on Active Experiments, 343, 1988.

Cohen, H.A., R.C. Adamo, T. Aggson, A.L. Chesley, D.M. Clark, S.A. Dameron, D.E. Delroy, J.F. Fennell, M.S. Gussenhoven, F.A. Hanser, D. Hall, D.A. Hardy, W.B. Huber, . Katz, H.C. Koons, S.T. Lai, B. Ledley, P.F. Mizera, A.G. Rubin,G.W. Schnulle. N.A. Saflekos, M.F. Tautz and E.C. Whipple, P78-2 Satellite and Payload Responses to Electron Beam Operations on March 30, 1979, in Spacecraft Charging Technology 1980, NASA CP 2182; AFGL-TR-81-0270, ed. by N.J. Stevens and C.P. Pike, 509-559, 1981. ADA114426

Linson, L.M., (1983) The Importance of Neutrals, Transient Effects and the Earth's Magnetic Field on Sheath Structure, in Proceedings of the Air Force Geophysics Laboratory Workshop on Natural Charging of Large Space Structures in Near Earth Polar Orbit: 14-15 September 1982, AFGL-TR-83-0046, ed. by R.C. Sagalyn, D.E. Donatelli and I. Michael, pp. 283-292, 1983. ADA134894

Maehlum, B.N., J. Troim, N.C. Maynard, W.F. Denig, M. Friedrich and K.M. Torkar, Studies of the electrical charging of the tethered electron accelerator mother-daughter rocket MAIMIK, Geophys. Res. Lett., 15, 725-728, 1988.

Massey, D.E., C.P. Williams, E.D. Ransone T.E. EDDY and S.J. Monson, Black Brant 36.004 UE Final Failure Report, NASA Goddard Space Flight Center, Wallops Flight Facility, 1987. Pierce, J.R., Theory and Design of Electron Beams, D. Van Nostrand Co., New York, 167 - 187, 1949.

Nemzek, R.J., ECHO 7 - Magnetospheric Properties Determined by Artificial Electron Beams, PhD thesis, University of Minnesota, Minneapolis, MN, 1990.

Nemzek, R.J., P.R. Malcolm and J.R. Winckler, Comparison of Echo 7 Electron Bounce Time Measurements to Magnetospheric Model Predictions, to be submitted to J. Geophys. Res., 1991.

Winckler, J.R., P.R. Malcolm, R.L. Arnoldy, W,J, Burke, K.N. Erickson, J. Ernstmeyer. R.C. Franz, T. J. Hallinan, P.J. Kellogg, K.A. Lynch, S.J. Monson, G.P. Murphy, and R.J. Nemzek, ECHO-7: An Electron Beam Experiment in the Magnetosphere, EOS: Trans. Am. Geophys. U., 70, 657-668, 1989.
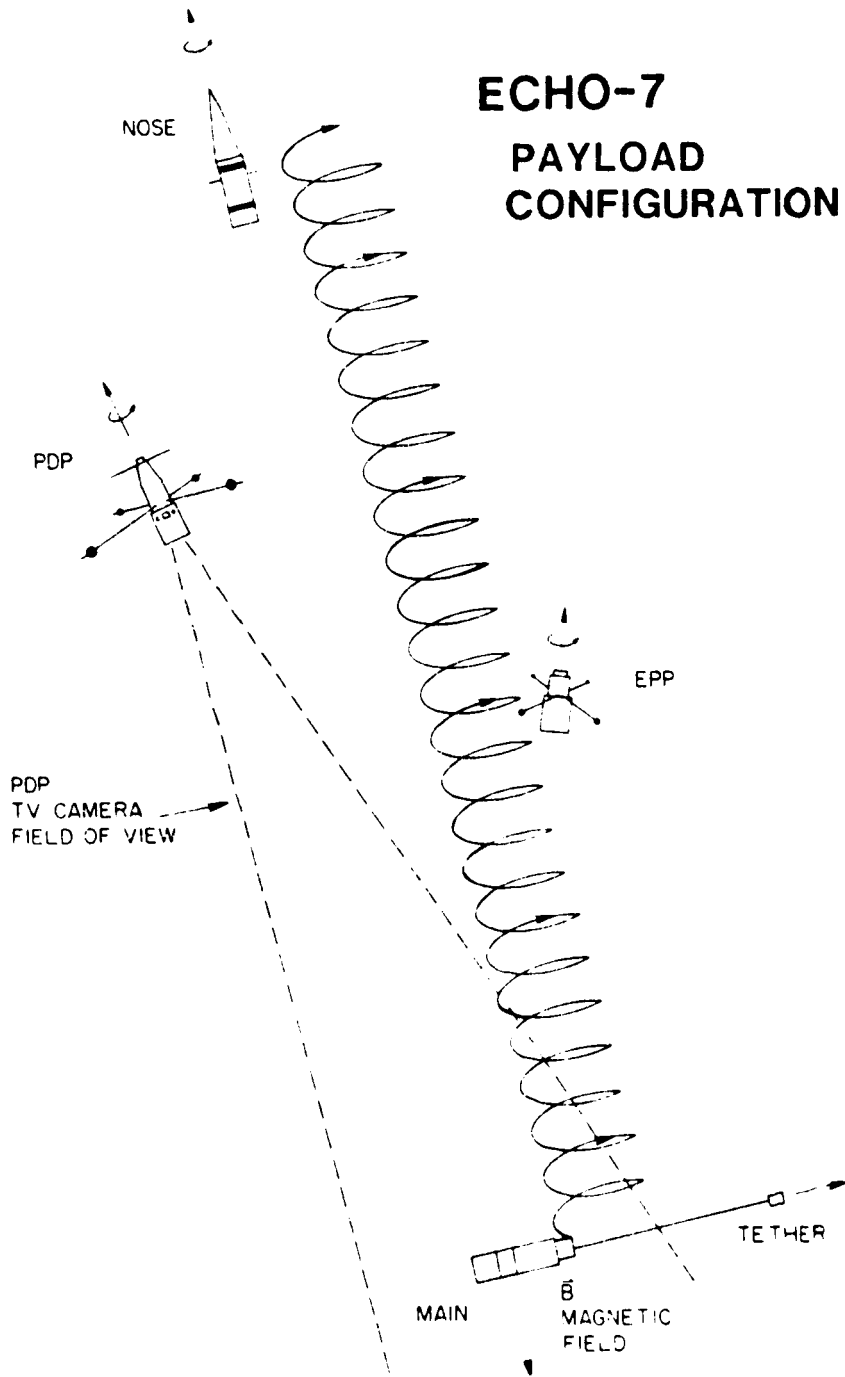
Figure 1.   Configuration of the four free-flying ECHO-7 payloads. NOSE was ejected straight up the magnetic field line, the Plasma Diagnostics Payload (PDP) 10° to the magnetic south and the Energetic Electron Payload (EPP) 25° to the magnetic west of the electron beam emitting MAIN payload.
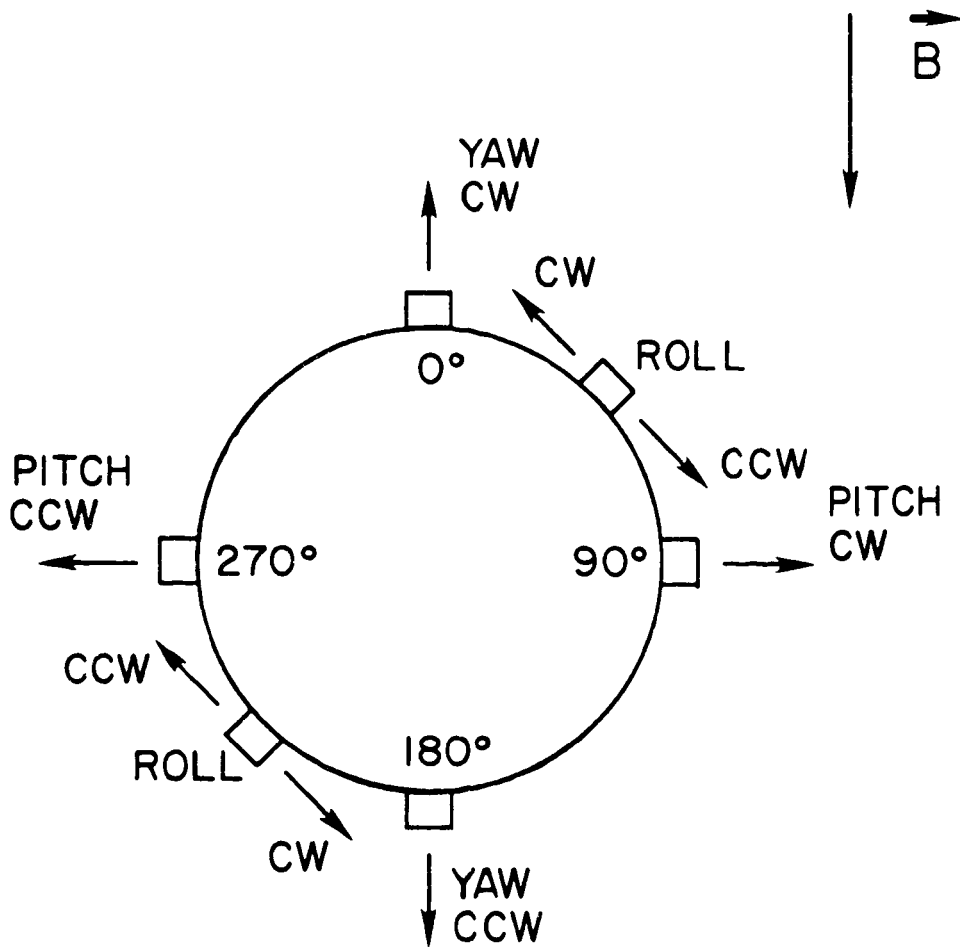
Figure 2. The relative positions of the pitch roll and yaw gas jet nozzles relative to the direction of the earth's magnetic field. The notations CW and CCW indicate clockwise and counter clockwise impulses applied to MAIN.
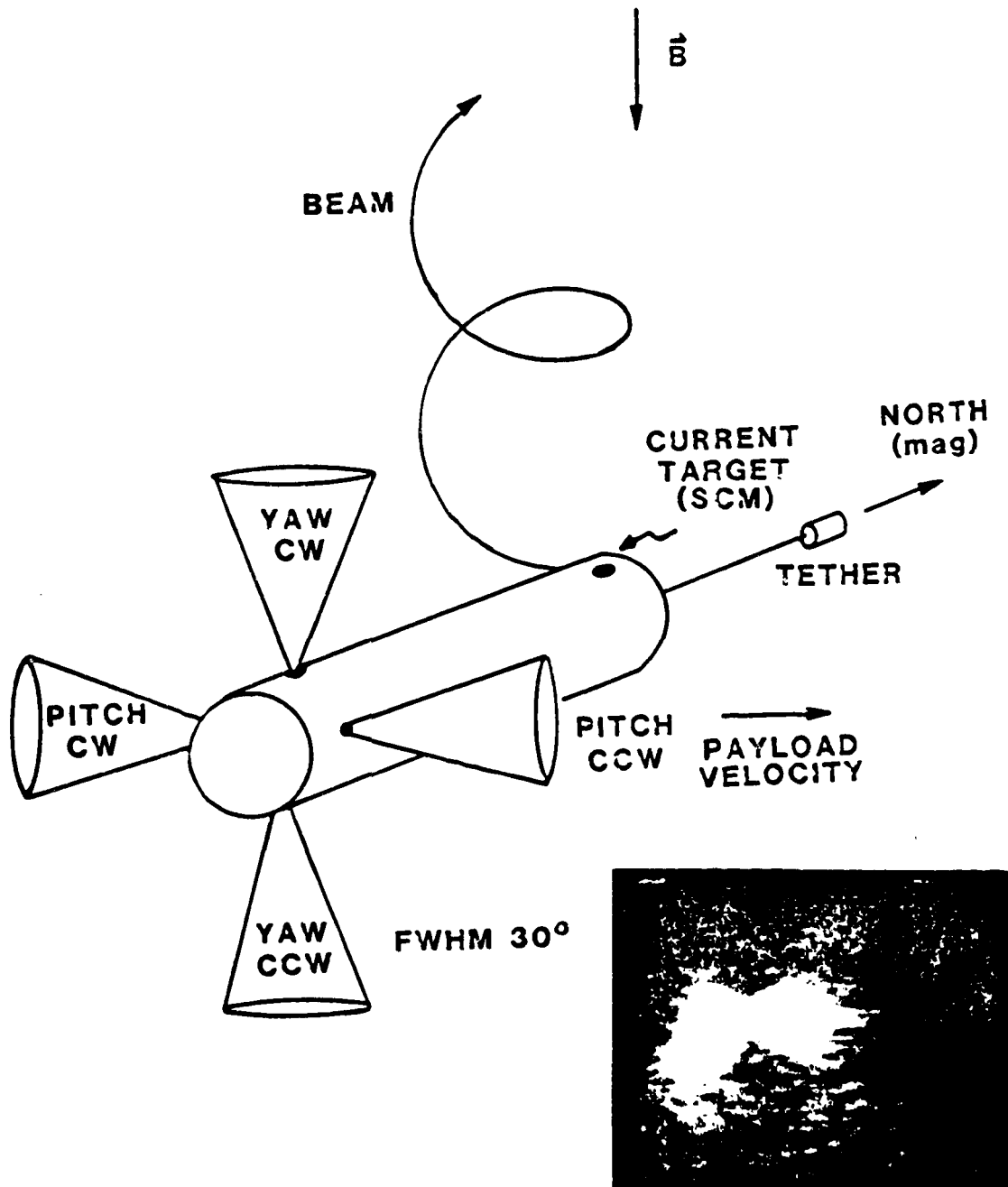
Figure 3. Configuration of the ECHO-7 MAIN payload, orientated perpendicular to the earth's magnetic field with the TETHER being ejected toward the magnetic north. The surface current monitor (SCM), or current target, was located on the top side of the payload near the electron gun. The attitude control system (ACS) was located on the south end of the payload with the orientations of pitch and yaw jets shown. The inset shows ACS roll jet nitrogen plumes, excited during beam emission, recorded by the PDP television camera.
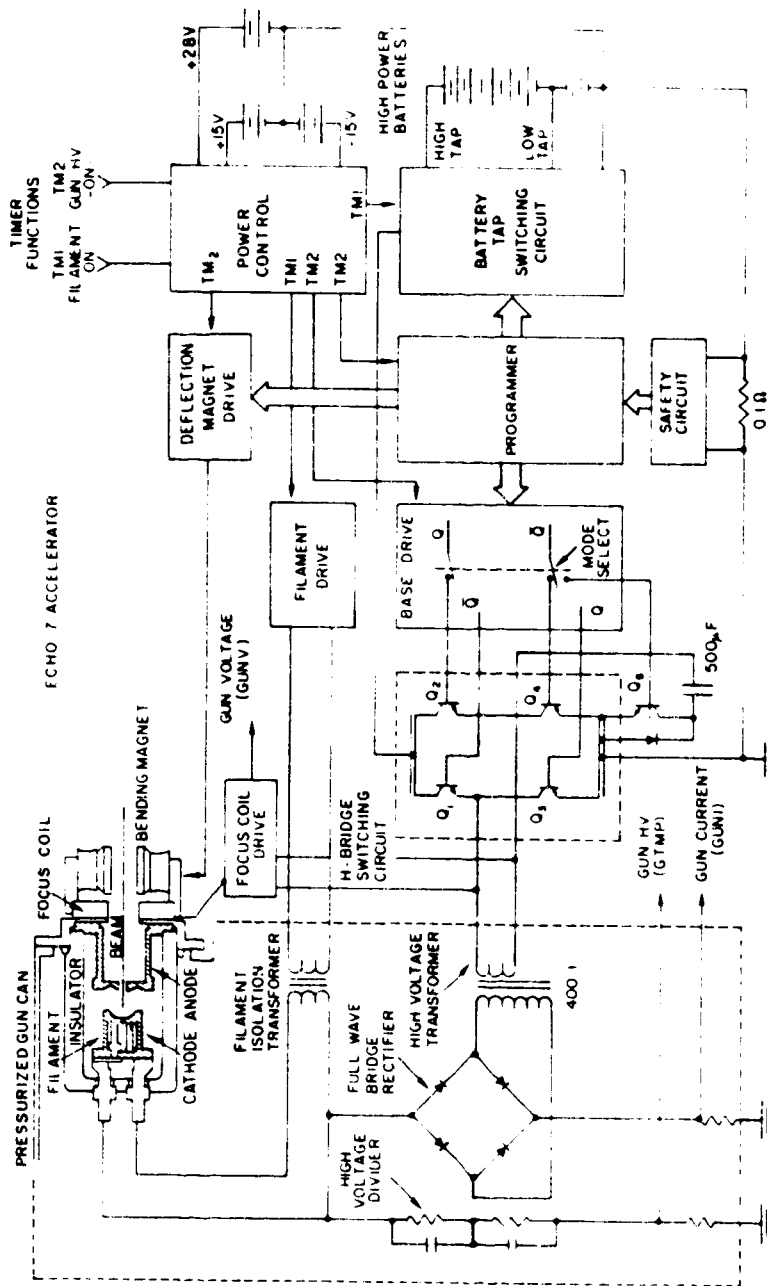
Figure 4. Diagram representing the main components of the ECHO-7 electron beam emission system.

ELECTRON GUN OUTPUT WAVEFORMS

DISCRETE BEAM

VOLTAGE
10.0 KV/DIV

0

CURRENT
62.5 MA/DIV

0

1.0 MSEC/DIV

CONTINUOUS BEAM

VOLTAGE
10.0 KV/DIV

0

CURRENT
62.5 MA/DIV

0

1.0 MSEC/DIV
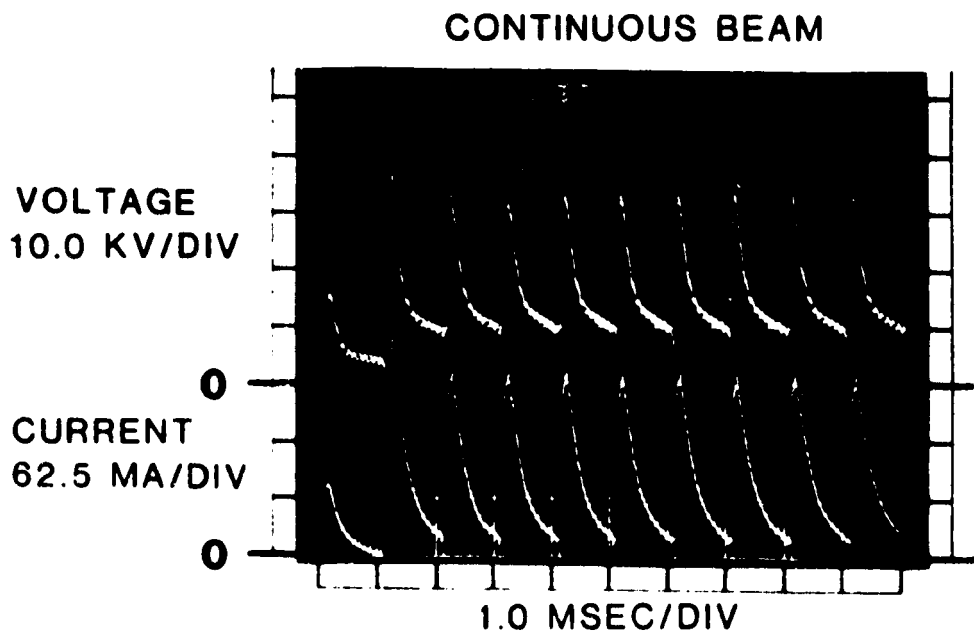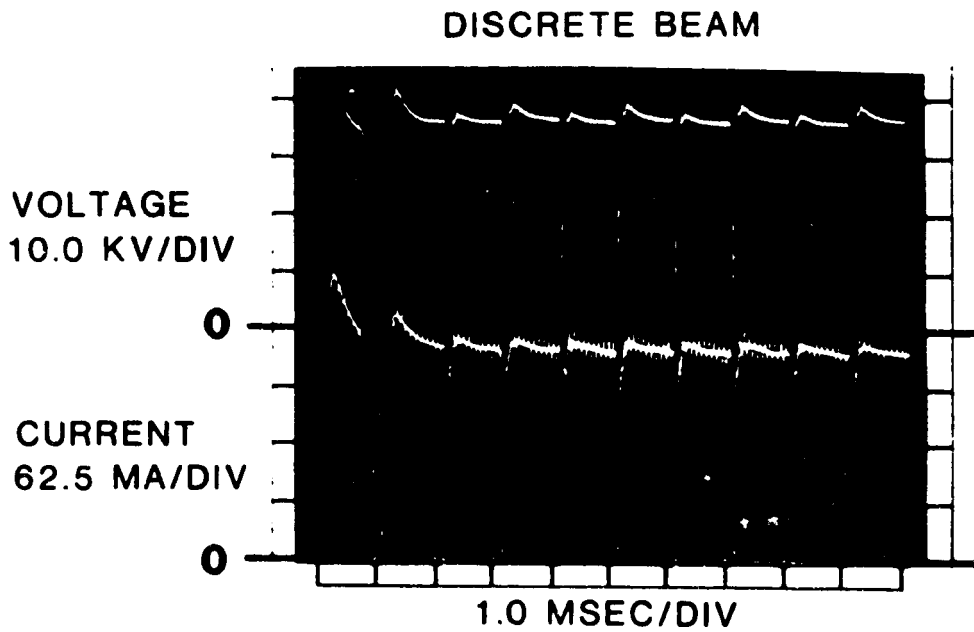
Figure 5. Oscilloscope photographs of accelerator output voltages and currents while operating in the "discrete" and "continuous modes".
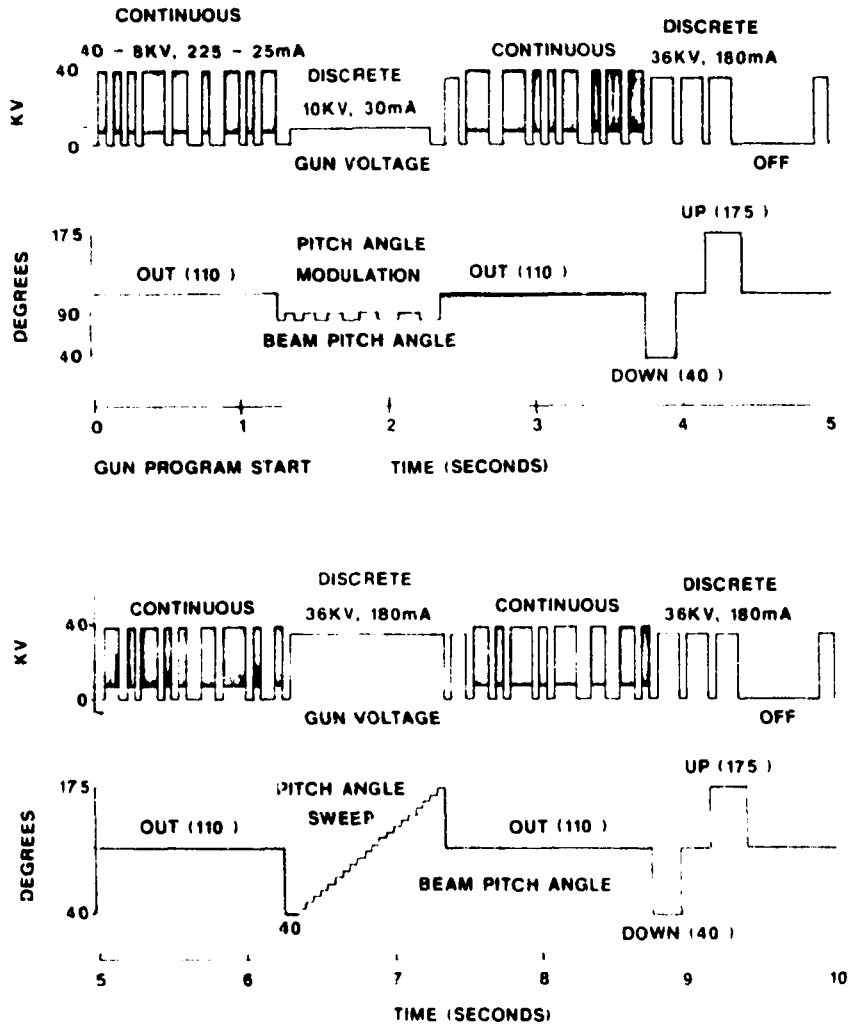
Figure 6. The ten-second, programmed electron beam emission sequence. This sequence was repeated from beam turn-on at 179 sec of the flight through re-entry at 500 seconds.
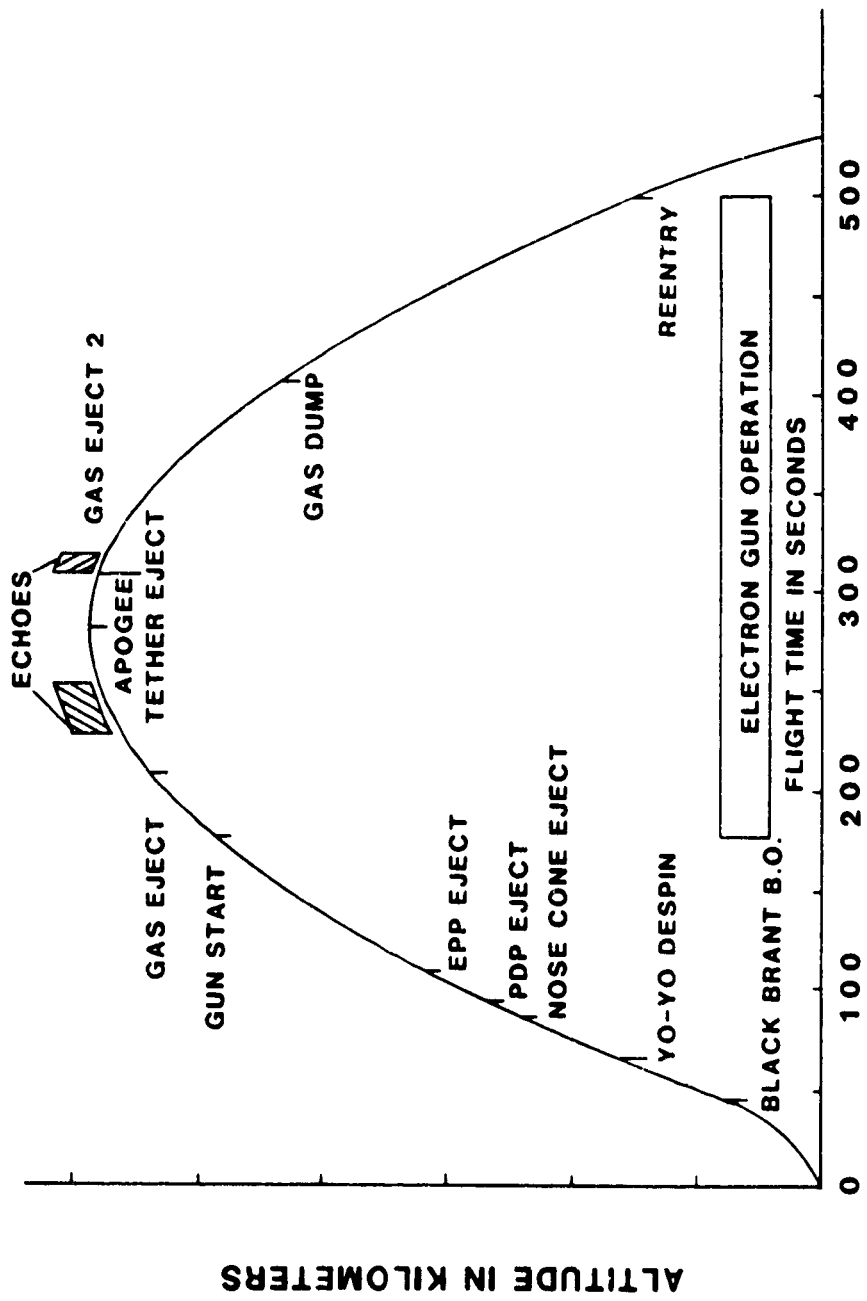
Figure 7. Time-altitude plot of ECHO-7 trajectory with time events labeled.
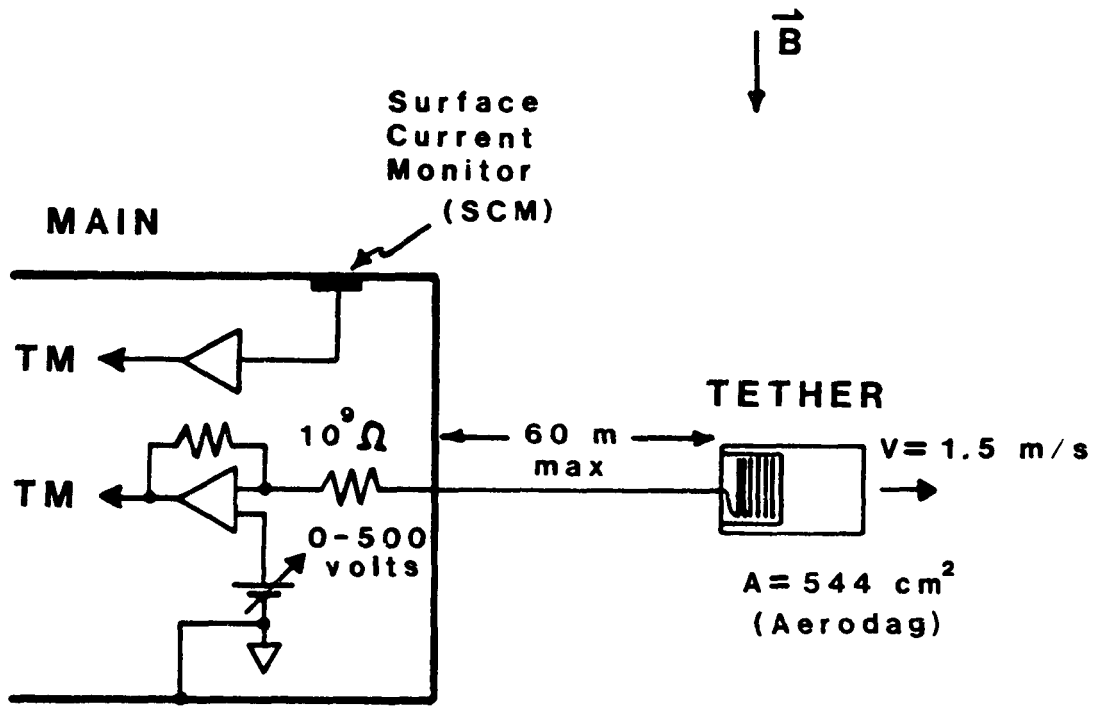
Figure 8. Schematic representing the TETHER deployment configuration and electronic circuitry.
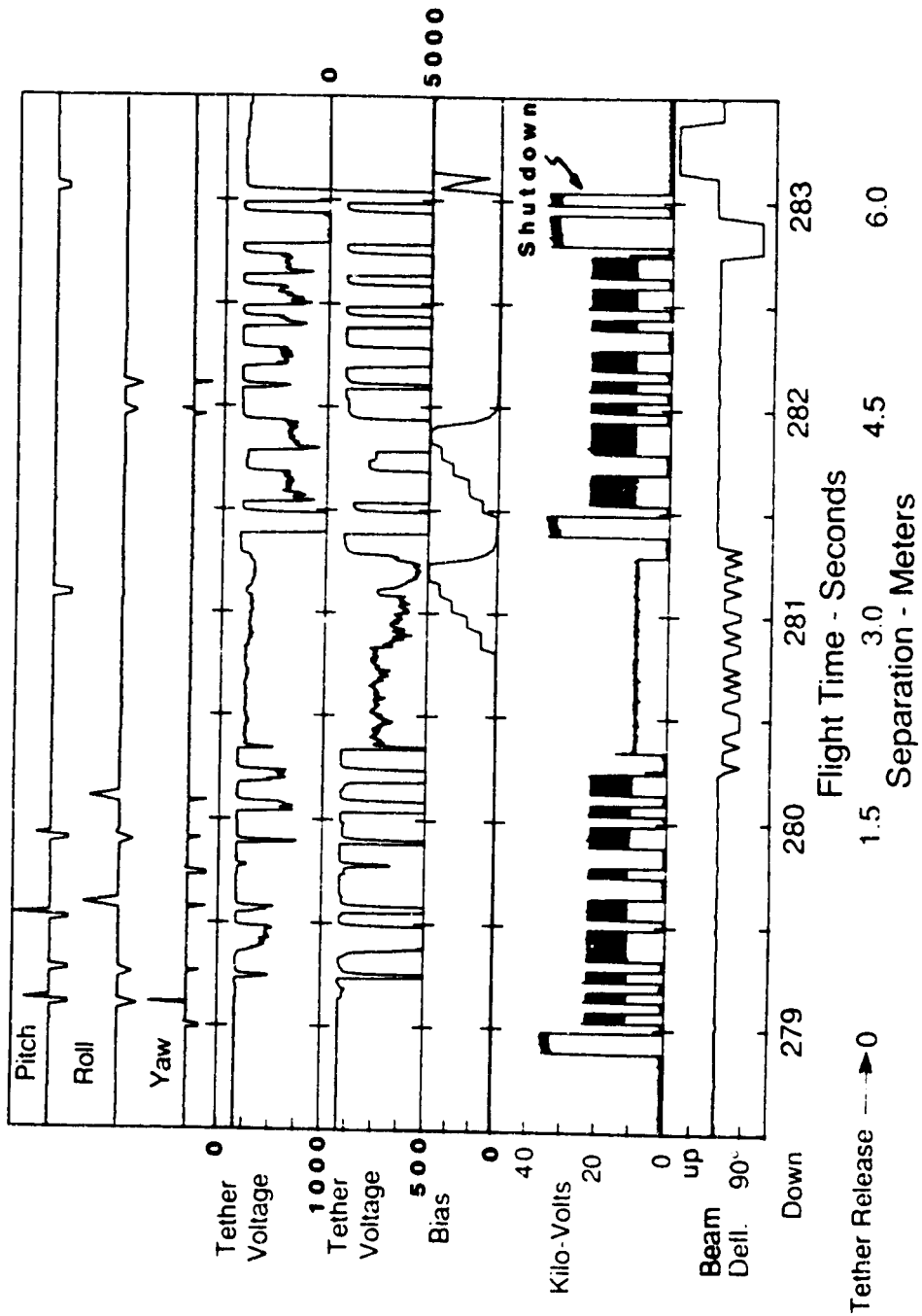
Figure 9. MAIN-Tether data acquired during the inte val 278.5 - 283.5 sec after launch. The top three panels give the ACS status. The next two panels give the Tether potential with respect to MAIN at two levels of sensitivity. The fifth panel shows the bias voltage applied to TETHER. The bottom two panels represent the beam voltages and injection pitch angles.
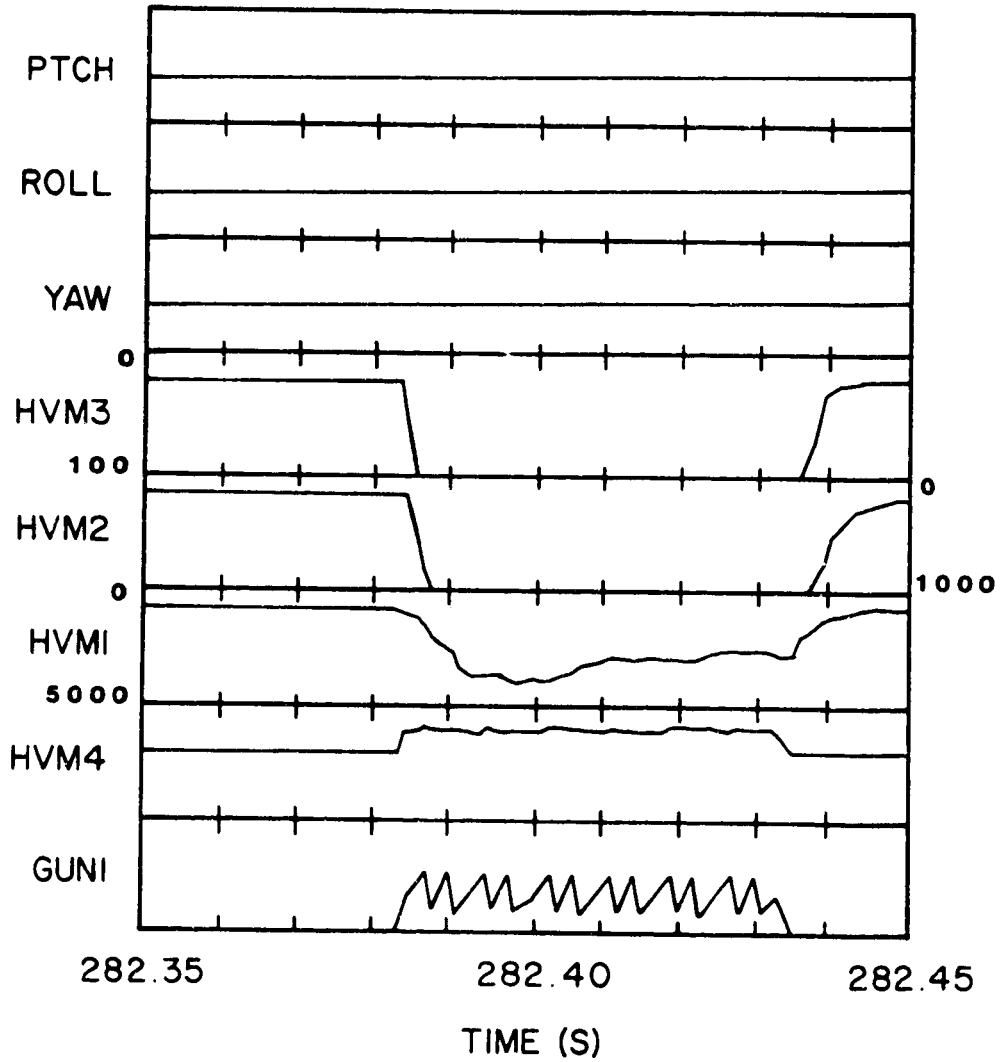
Figure 10. MAIN/TETHER measurements during a 50 ms continuous beam operation with no ACS ejection.
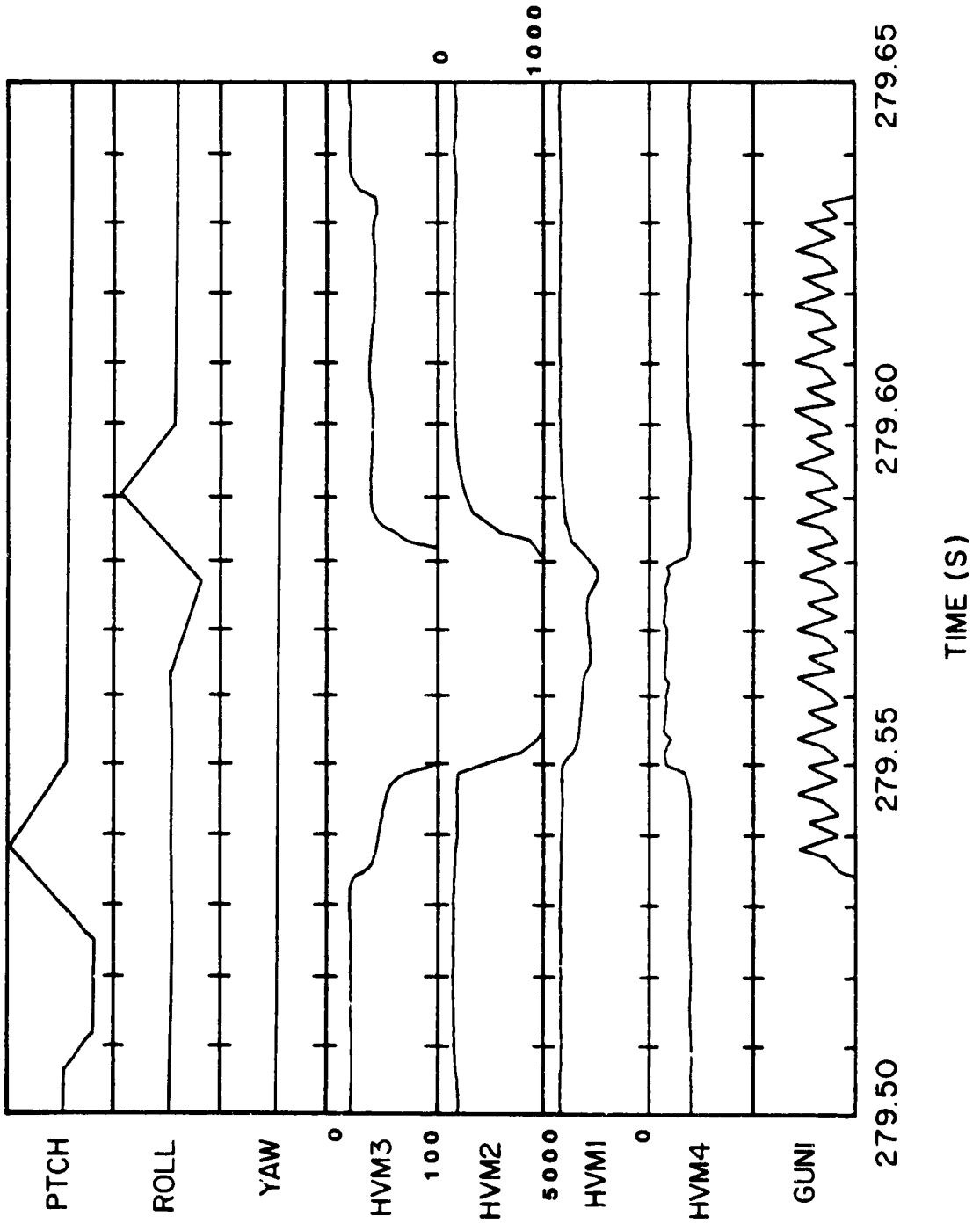
Figure 11.   MAIN-TETHER measurements during a 100 ms
continuous beam operation with a sequence of pitch and roll
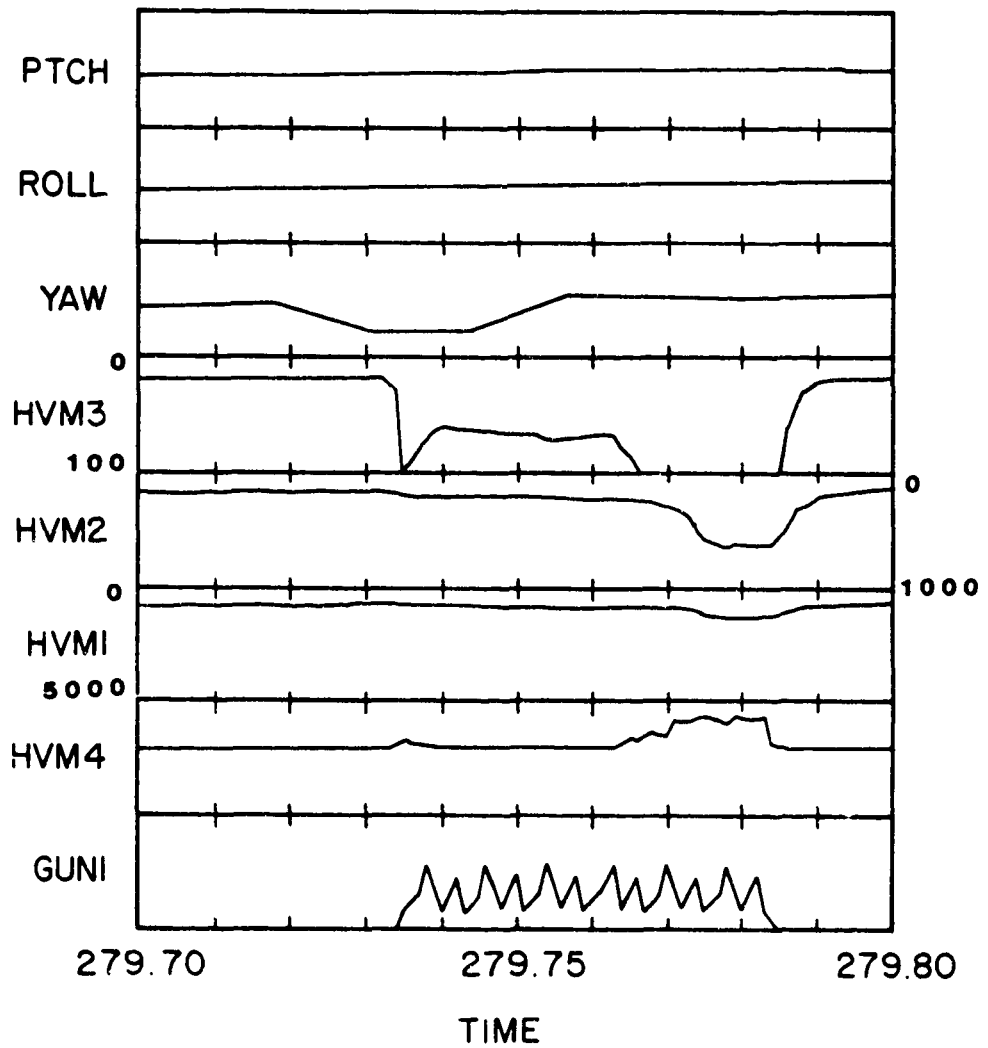ACS ejections.

Figure 12.   MAIN-TETHER measurements during a 50 ms
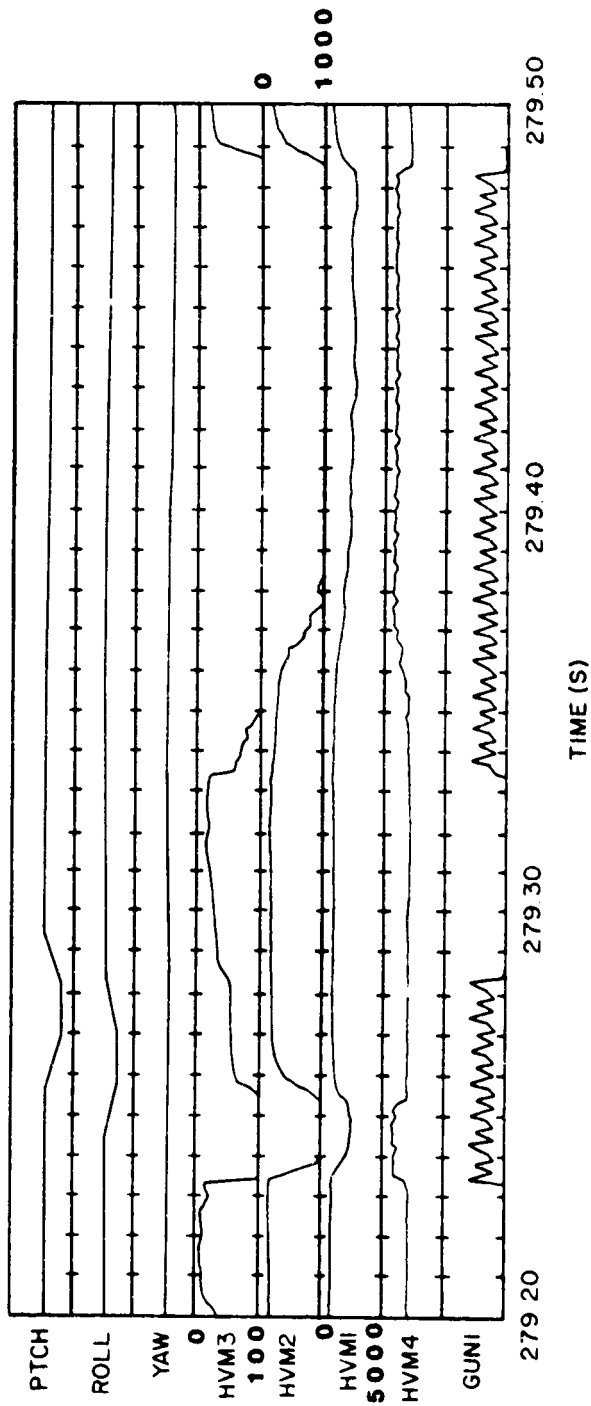continuous beam operation with a yaw ACS ejection.

Figure 13. MAIN-TETHER measurements during a sequence of continuous operations with a pitch and roll ACS operation.
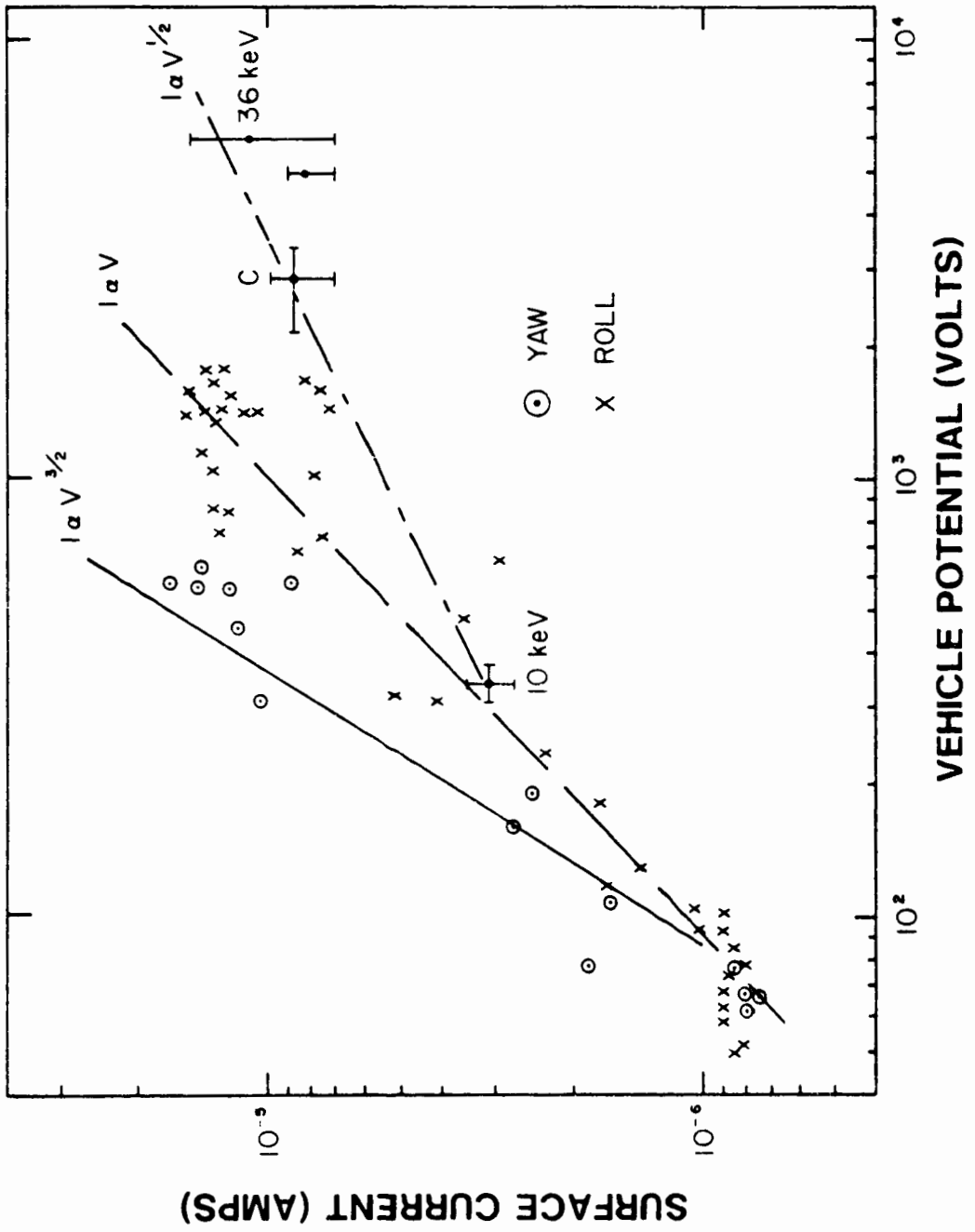
Figure 14. Surface current measurements as a function of the vehicle potential. The circled dots (crosses) represent measurements after the yaw (roll) gas ejections shown in Figure 8.